

Merging of Components in Close Binaries: Type Ia Supernovae, Massive White Dwarfs, and Ap stars

A. I. Bogomazov¹, A. V. Tutukov²

¹ *Sternberg Astronomical Institute, Moscow State University,
Universitetski pr. 13, Moscow, 119992, Russia,*

² *Institute of Astronomy, Russian Academy of Sciences,
ul. Pyatnitskaya 48, Moscow, 109017, Russia*

Astronomy Reports, volume 53, no. 3, pp. 214-222 (2009)

The “Scenario Machine” (a computer code designed for studies of the evolution of close binaries) was used to carry out a population synthesis for a wide range of merging astrophysical objects: main-sequence stars with main-sequence stars; white dwarfs with white dwarfs, neutron stars, and black holes; neutron stars with neutron stars and black holes; and black holes with black holes. We calculate the rates of such events, and plot the mass distributions for merging white dwarfs and main-sequence stars. It is shown that Type Ia supernovae can be used as standard candles only after approximately one billion years of evolution of galaxies. In the course of this evolution, the average energy of Type Ia supernovae should decrease by roughly 10%; the maximum and minimum energies of Type Ia supernovae may differ by no less than by a factor of 1.5. This circumstance should be taken into account in estimations of parameters of acceleration of the Universe. According to theoretical estimates, the most massive – as a rule, magnetic – white dwarfs probably originate from mergers of white dwarfs of lower mass. At least some magnetic Ap and Bp stars may form in mergers of low-mass main-sequence stars ($M \lesssim 1.5M_{\odot}$) with convective envelopes.

1 Introduction

Here, we consider the role of component mergers in various close binaries in the formation of some astrophysical objects and the generation of one of the greatest natural phenomena – Type Ia supernovae (SN Ia).

Currently, the most popular explanation for SN Ia is mergers of two carbon-oxygen white dwarfs (CO WDs) under the action of gravitational radiation, provided the total mass of the merging dwarfs exceeds the Chandrasekhar limit. This scenario for the formation of SN Ia was suggested in the early 1980s (see, for example, [1, 2]). Up to 40% suggesting that their progenitors may form an inhomogeneous group of objects [3]. Apart from mergers of two CO dwarfs, possible origins include the thermonuclear explosion of a WD in a semi-detached system during the accretion of matter from its companion, when the dwarf’s mass exceeds the Chandrasekhar limit [4], and a thermonuclear explosion of a white dwarf with a helium donor star companion; under certain conditions, the mass of the WD may be lower than the Chandrasekhar limit [5]. Here, however, we consider

the basic scenario for the formation of SN Ia to be the merging of two CO dwarfs whose total mass exceeds the Chandrasekhar limit. The high age dispersion of SN Ia precursors, $\sim 10^8 - 10^{10}$ years [6] supports this scenario. The conditions for an SN Ia explosion have also been considered, for example, in [7].

At the end of the twentieth century, observations of distant SN Ia resulted in the discovery that the expansion of the Universe is accelerating [8, 9]. It was suggested that SN Ia can be used as standard candles, and that their magnitudes at the maximum brightness can be determined from the slope of the light curve, according to the regular trends revealed by Pskovskiy [10]. Taking into account the most popular SN Ia model, we suggest that the use of this type of supernova as standard candles may encounter an obvious problem: the total mass of the merging WDs may only slightly exceed the Chandrasekhar limit, or be only a little lower than two Chandrasekhar limits. In this case, the scatter of SN Ia maximum luminosities could reach a factor of two. Average total mass of the merging dwarfs decreases with time imitating accelerated expansion of the Universe. Additional uncertainty is introduced by the fact that current concepts do not exclude the possibility of a thermonuclear explosion of two merged degenerate dwarfs whose total mass is somewhat below the Chandrasekhar limit.

Optical observations of SN Ia revealed some inhomogeneity in their properties. A subtype with lower luminosities, and probably lower energy releases, can be distinguished (for example, [11]). It remains unclear if this subtype is associated with a decreased abundance of heavy elements or a lower mass of the pre-supernova. SN Ia may also differ somewhat in the expansion velocities of their envelopes [12]; again, it is unclear whether this is due to different explosion energies or, for example, different orientations of the supernova envelope relative to the observer [13]. The increase in the frequency of SN Ia explosions at early stages in the evolution of galaxies [14], when the star formation rate was higher than its present value [15], provides evidence that relatively short-lived objects with lifetimes of about $1 - 2 \cdot 10^9$ years are also among SN Ia progenitors. However, in most cases, SN Ia progenitors have longer lifetimes [16]. Some SN Ia are embedded into circumstellar envelopes that are expanding with velocities of up to 50 km/s [17], suggesting that these supernovae evolved from symbiotic binaries with red-giant donors. This model was suggested, for example, in [18] to explain novae outbursts, and in [4] to explain Type I supernovae, which at that time were not yet divided into the Ia, Ib, and Ic subtypes. A scenario in which degenerate components of close binaries merge under the action of gravitational waves is also possible, though unlikely, in this case. The observed envelopes are then the remnants of the common envelopes, which “dissolve” in the interstellar medium on time scales of $\sim 10^5$ years.

In order to investigate the “standardness” of SN Ia, we have calculated the rates of mergers of degenerate dwarfs with various chemical compositions, constructed the mass functions of merging WDs, and derived the average mass of merging dwarfs as a function of the time since the onset of star formation in a galaxy under various assumptions concerning the star-formation history. We also consider the results of merging two WDs with a total mass below the Chandrasekhar limit and of degenerate dwarfs with various masses and ages.

The magnetic fields of non-interacting magnetic white dwarfs (MWDs) lie in the interval 0.1-1000 MG, with the peak in the distribution around 16 MG (see the review [19]). It

is commonly believed that MWDs are the remnants of magnetic Ap and Bp stars. There are also some indications that the MWD mass function is bimodal, with a second maximum close to the Chandrasekhar limit. This maximum could correspond to mergers of degenerate dwarfs. The rotational velocities MWDs are also bimodal: they include both rapidly rotating stars with rotational periods from roughly 700 s to several hours, as well as virtually non-rotating MWDs, for which formal estimates of their rotational periods yield values of the order of 100 years. The rapidly rotating MWDs are naturally thought to arise from mergers of WD components in close binaries. In addition, their rotation may have been substantially accelerated by accretion during their evolution in a close binary. Slow MWDs have most likely evolved from stars (either single, or components of wide binaries) whose cores were strongly magnetized and lost their angular momentum during interaction with the extended envelope of the star. It can also not be excluded that the magnetic field strongly affects the initial “mass-radius” relation, and thus the consequences of the evolution of close binaries, such as the SN Ia rate (see [19]).

A catalog of 112 massive (with masses $\geq 0.8M_{\odot}$) WDs (both single and binary) that do not interact with other stars is presented in [20]. The mass distribution for these dwarfs is generally continuous, and decrease fairly rapidly with increasing mass. Massive WDs with strong magnetic fields display an almost flat mass distribution. Note that the four most massive WDs (with masses $\geq 1.3M_{\odot}$) are magnetic. The presence of a magnetic field is not correlated with the temperature (and probably also not with the age) of the white dwarf: magnetic and non-magnetic degenerate dwarfs have the same temperature distributions [20]. Table 1 in [20], shows that 3 of 25 MWDs are components of binaries. Only one of these three dwarfs (EUVE J0317-855) is among the most massive; it is situated in a very wide system, with an approximate component separation of 1000 AU (see, for example, [21]); consequently, these stars have never interacted. The high rotational velocity, high mass, and an age inconsistent with the suggested companion (the WD LB 9802) suggest that EUVE J0317-855 may be the result of a merger of two WDs [19, 22, 23].

Mergers of rotating, close, binary, stellar-mass black holes yield peculiar consequences [24, 25]. Modeling has shown that the black holes formed as a result of the merger can acquire velocities of several thousands of km/s. These stars subsequently leave not only their parent galaxies, but also the clusters of galaxies to which they belong. Such black holes can have covered distances of ≈ 50 Mpc over the Hubble time. Thus, they form a kind of continuous medium filling the space between clusters of galaxies located at distances of up to 35-70 Mpc [26]. We have calculated the rates of mergers of neutron stars (NSs) with WDs and with black holes (BHs). Our aim was to obtain theoretical merger rates for various compact objects (WDs, NSs, BHs), using the same computer code (the “Scenario Machine”) to carry out population syntheses for the same sets of parameters of the evolutionary scenario. A thorough study of mergers of NSs with NSs and BHs and of the impact of various parameters of the evolutionary scenario on these events are presented, for example, in [27, 28].

The current state of studies of the evolutionary status of Ap and Bp stars is described in detail in [29]. We are primarily interested in the occurrence rate for magnetic Ap stars among all A stars. Roughly, $R = \frac{N(Ap)}{N(Ap)+N(A)}$ (here, $N(Ap)$ is the number of magnetic Ap stars and $N(A)$ the number of A stars). If we restrict the volume in which this relation is measured, R becomes equal to 0.01-0.02 [30]. Here, we suggest that magnetic Ap stars

are the products of mergers of components in close binaries with convective envelopes due to the action of the magnetic stellar wind (MSW)¹. In this case, the maximum and minimum initial semimajor axes in such systems are $a_{max}/R_{\odot} \simeq 7.25M/M_{\odot}$ and $a_{min}/R_{\odot} \simeq 6(M/M_{\odot})^{1/3}$ ([31]), where M is the mass of each of the binary components, assumed for this estimate to be equal. Only components in close binaries for which the initial masses of each component exceed $\approx 0.75M_{\odot}$ (with a total mass of $\approx 1.5M_{\odot}$) can merge. The interval of semimajor axes in the merging systems increases from zero for $M \approx 0.75M_{\odot}$ to $7 - 11R_{\odot}$ for $M = 1.5M_{\odot}$. The latter can be estimated using the following equation describing the loss of orbital angular momentum of the system via the MSW (see Eq. (34) in [31]):

$$\frac{d \ln J}{dt} = -10^{-14} \frac{R_2^4 (M_1 + M_2)^2 R_{\odot}}{\lambda^2 a^5 M_1 M_{\odot}} \text{s}^{-1}, \quad (1)$$

where M_2 and R_2 are the mass and radius of the component with the MSW, M_1 is the mass of the secondary, a is the semimajor axis of the orbit, and λ is the MSW parameter (assumed to be unity). The above interval for the semimajor axes corresponds to a rate of formation of Ap stars of several per cent of the total number of stars with initial masses exceeding $\sim M_{\odot}$. In this scenario, the strong magnetic fields of the progenitors of Ap stars explain the presence of strong fields in Ap stars. The equatorial rotational velocities of magnetic Ap stars for $R \simeq 2R_{\odot}$ and $P_{orb} = 0.5 - 5$ day are $20 - 200$ km/s; i.e., they can be high. Note also that the low rotational velocity displayed by many Ap stars does not unambiguously argue against the possible formation of Ap stars as a result of mergers of main-sequence stars with convective envelopes, since angular momentum could be lost together with some of the matter in the course of the merger.

2 Population synthesis

The principles of the ‘‘Scenario Machine’’ have been described repeatedly, and we will restrict our consideration to the selection of the free parameters of the evolutionary scenario. A detailed description of the code is presented in [27, 32, 33].

For each set of evolutionary-scenario parameters, we carried out a population synthesis for 10^6 binaries. The rates of events and the numbers of objects in the Galaxy are obtained, assuming that all stars are binary. In our study, we took as free parameters the efficiency of the common envelope stage, α_{CE} , and the additional kick velocity acquired during the formation of neutron stars and black holes.

2.1 Kick Acquired in a Supernova Explosion

We assumed that the NS or BH that forms during a supernova explosion can acquire a kick velocity v , which is random and has a Maxwell distribution:

$$f(v) \sim \frac{v^2}{v_0^3} e^{-\frac{v^2}{v_0^2}}, \quad (2)$$

¹We will consider the magnetic stellar wind only from the primary (more massive) component

with all directions for the kick being equally probable. The characteristic velocity v_0 , acquired by the remnant is one of the critical parameters for estimating the birth rates for systems that remain bound after the supernova explosions in them. Naturally, the results of the population synthesis strongly depend on v_0 . Increasing v_0 to velocities above the orbital velocities in close binaries (~ 100 km/s) results in a dramatic decrease in the number of systems containing relativistic components [28]. Note, however, that this kick can not only disrupt, but also bind some systems that would have decayed without it.

It is believed that the magnitude of the kick velocity acquired during the formation of a BH depends on the fraction of mass lost by the star in the supernova explosion. We assume that a star loses half its mass in the explosion [34]. Thus, for a BH, we take the characteristic kick velocity v_0 and obtain the velocity v , according to the distribution (2), which we divide by two.

2.2 Mass-loss Efficiency in the Common-Envelope Stage

During the common-envelope stage, stars transfer angular momentum to the adjacent matter of the envelope very efficiently in course of spiral-in. The efficiency of the mass loss in the common-envelope stage is described by the parameter $\alpha_{CE} = \Delta E_b / \Delta E_{orb}$, where $\Delta E_b = E_{grav} - E_{thermal}$ is the binding energy of the ejected envelope matter and ΔE_{orb} is the decrease in the orbital energy of the system as the stars approach [31, 35]. Thus, we obtain

$$\alpha_{CE} \left(\frac{GM_a M_c}{2a_f} - \frac{GM_a M_d}{2a_i} \right) = \frac{GM_d(M_d - M_c)}{R_d}, \quad (3)$$

where M_c is the core mass of the mass-losing star, which has an initial mass M_d and radius R_d (which is a function of the initial semimajor axis a_i and the initial mass ratio M_a/M_d , where M_a is the mass of the accretor).

2.3 Other Parameters of the Evolutionary Scenario

In this Section, we present values for some parameters of the evolutionary scenario. The maximum mass of a NS that can be reached in the course of accretion (the Oppenheimer-Volkov limit), was taken to be $M_{OV} = 2.0M_\odot$, while the initial masses of young NSs were randomly distributed in the interval $1.25 - 1.44M_\odot$. We assumed that main sequence stars with initial masses in the interval $10 - 25M_\odot$ end their evolution as NSs. We augmented the progenitors of NSs with main sequence components of close binaries that increase their mass as a result of mass transfer, after which their mass reaches the above interval. More massive stars ultimately evolve into BHs, and less massive stars into WDs. In the calculations carried out here, we adopted an equiprobable (flat) distribution for the component mass ratios of the initial binaries [31] and a zero initial eccentricity for their orbits. All the calculations presented here assume a classical weak stellar wind (see [32], and also the A evolutionary scenario in [34]). We also adopted a flat distribution for the initial semimajor axes in the binaries $d(\log a) = \text{const}$ in the interval $5 - 10^6 R_\odot$.

3 Results

Table 1 presents the birth and merger rates for WDs with various chemical compositions, as well as the rates for WD mergers with NSs and BHs, calculated for various mass loss efficiencies in the common-envelope stage α_{CE} . Table 2 contains the rates of mergers of NSs with NSs and BHs for various characteristic kick velocities acquired during the formation of the NSs (v_0) and BHs (v_0^{bh}). The rates of events in Tables 1 and 2 are calculated for a galaxy with a total mass of stars and gas of $10^{11}M_\odot$ and a star formation rate specified by the Salpeter function.

Figures 1a-d present the WD mass distributions. The solid curve presents the distributions for WDs that have not undergone a merger, and the dash-dotted curve the total mass distribution for merging WDs. Figure 1a shows the distributions for WDs of all chemical compositions, Fig. 1b for helium WDs, Fig. 1c for carbon-oxygen WDs, and Fig. 1d for oxygen-neon WDs. Figure 1e plots the total mass distribution for merging WDs with various chemical compositions: the solid curve indicates mergers of oxygen-neon WDs with carbon-oxygen WDs, the dash-dotted curve mergers of oxygen-neon WDs with helium WDs, and the dotted curve mergers of carbon-oxygen WDs with helium WDs.

Figures 2a-c present the average mass of merging WDs as a function of the time since the onset of the formation of these stars. Depending on the mass of the formed binary WD and the semimajor axis of the WD binary, the time until the merger due to the action of gravitational waves can range from several tens of million years up to the Hubble time. The number of mergers of WDs $N_\delta(t)$ was calculated assuming all stars in a galaxy are born simultaneously (with the star formation rate represented by a δ function). The evolution of this quantity in a galaxy with arbitrary star formation is specified by the formula

$$N(t) = \int_0^t N_\delta(t - \tau)\varphi(\tau) d\tau, \quad (4)$$

where $N(t)$ is the number of mergers as a function of time t since the onset of star formation and $\varphi(t)$ a function describing the star-formation history. The average mass of merging dwarfs $\overline{M}(t, t + \Delta t)$ is given by

$$\overline{M}(t, t + \Delta t) = \frac{\sum_i M_i}{N(t, t + \Delta t)}, \quad (5)$$

here M_i are sums of the masses of WDs merging at a time in the interval t to $t + \Delta t$. Figure 2a presents the average masses of merging WDs calculated assuming that all stars in the galaxy form simultaneously (the function $N_\delta(t)$, calculated using the ‘‘Scenario Machine’’); a constant star formation rate was assumed in Fig. 2b; the star formation history presented in [36] was used to construct the curves in Fig. 2c; the numbers of mergers for the graphs in Fig. 2 band 2c were calculated using (4). The numbers in Figs 2a-2c denote the average masses of 1 all merging WDs, 2 merging WDs with all possible chemical compositions (but including only mergers in which the total mass of the WDs

exceeds the Chandrasekhar limit), 3 carbonoxygen WDs, 4 carbon-oxygen WDs whose total mass exceeds the Chandrasekhar limit.

The time since the formation of a binary WD system that can later merge due to the radiation of gravitational waves depends on the masses of the WDs in the system, as well as the semimajor axis of the system. Figure 3 presents the dependence of the number of mergers of carbon-oxygen WDs whose total masses exceed the Chandrasekhar limit on the time since the formation of the close binary containing two CO dwarfs.

Figure 4 presents the mass distribution for Ap stars, here considered to be main sequence stars formed in mergers of main sequence stars with convective envelopes under the action of the magnetic stellar wind. Most of these have masses in the interval $1.7 - 2.5M_{\odot}$.

4 Conclusion

We can see from Fig. 1a that the number of WDs with low masses ($\lesssim 1M_{\odot}$) originating due to mergers² is substantially smaller than the number of WDs that have never undergone merging. The mass distribution for WDs that are the end products of stellar evolution rather than of mergers of other WDs rapidly decreases towards higher mass, while the mass distribution for merging WDs with masses exceeding the solar value is essentially flat. The numbers of WDs originating in mergers and WDs that have not undergone merging become roughly equal for masses near $1.1M_{\odot}$. Naturally, at the highest masses ($\approx 1.3M_{\odot}$), the number of WDs that form due to merging exceeds the number that have never undergone merging by roughly a factor of ten. This result is in good consistency with the observations: on average, MWDs are more massive than WDs in general, and the number of magnetic stars among the most massive dwarfs is an order of magnitude higher than the number of non-magnetic stars [37]. When comparing Figs. 2 and 3 in [20], we see also that MWDs dominate in the mass distributions for magnetic and non-magnetic WDs with masses $\approx 1.2 - 1.3M_{\odot}$ though the statistics are fairly poor. Figures 1d and 1e show that the main contribution to the total mass distribution in the interval $1.1 - 1.4M_{\odot}$ is made by mergers of carbon-oxygen WDs, with a small contribution also made by mergers of oxygen-neon with carbon-oxygen WDs. Thus, we conclude that nearly all of the most massive MWDs originated as a result of mergers of close binary degenerate dwarfs.

Figures 2a-2c show that the average mass of merging WDs (without dividing them into different types according to their chemical composition) decreases rapidly with the age of the population, from $\approx 2.1M_{\odot}$ to less than $1M_{\odot}$. However, the average mass of merging WDs whose total mass exceeds the Chandrasekhar limit decreases rapidly from the maximum value to ($\approx 1.8 - 1.9M_{\odot}$), after which it remains nearly constant with time. The same pattern is observed if we restrict our consideration to the most popular candidate SN Ia progenitors – mergers of carbon-oxygen dwarfs with carbon-oxygen dwarfs. In a young galaxy, the average total mass of merging CO dwarfs is about $1.9M_{\odot}$. For times $\lesssim 1 \cdot 10^9$ years, this decreases to $1.6 - 1.7M_{\odot}$ then remains the same for the subsequent 13 billion years of evolution. Thus, we conclude that SN Ia can be used as

²With the total mass of the merging dwarfs below the Chandrasekhar limit.

standard candles only in galaxies older than approximately one billion years. If we assume that star formation begins at redshift³ $z=10$, then the average total mass of merging CO dwarfs will stop decreasing only at redshifts z of about two to three. This conclusion does not depend on our selection of star-formation functions (from those considered in the present study). Figure 1c indicates that the maximum mass of merging CO dwarfs is roughly $2.1M_{\odot}$, which exceeds the Chandrasekhar limit by a factor of 1.5. If we suppose that the energy release at the time of the thermonuclear explosion of the merged dwarfs is proportional to the mass, we expect that the scatter in the brightnesses of SN Ia at their maximum luminosity is also roughly a factor of 1.5 (or $0^m.5$). The conclusion that expansion of the Universe was accelerating reported in [8, 9] (Figures 4 and 5 in [8] and Figure 2 in [9]) was based on observations of SN Ia at distances of up to $z \sim 1$. The errors in the supernova brightnesses in these studies are about $0^m.5$. Consequently, the evolution of the average total mass of merging WDs and the scatter of the total mass about the average could not substantially affect the main conclusions of [8, 9]. However, it is essential to take into account described decrease of the total mass of merging white dwarfs with time in accurate estimations of parameters of acceleration of the Universe. Chemical composition variations may introduce additional scatter into the brightnesses of distant, “young” SN Ia; however, the present estimates of this effect suggest that this factor can be neglected [38].

Figure 3 indicates that the minimum time for two carbon-oxygen WDs whose total mass exceeds the Chandrasekhar limit to merge is roughly 90 thousand years. During the first million years of their lives, roughly 1% of such binary CO dwarfs merge. Consequently, in most cases, the envelopes of SN Ia (considered in [17]) cannot consist of matter ejected by the stars during the common-envelope stage, and the formation of SN Ia via the merging of two CO dwarfs in systems with envelopes is unlikely.

According to our calculations, the rate of mergers of main sequence stars under the action of the magnetic stellar wind for masses from $0.75M_{\odot}$ to $1.5M_{\odot}$ is roughly 0.0037/year in the Galaxy, while the total number of main-sequence stars in the Galaxy formed due to mergers for masses from 1.5 to $3M_{\odot}$ is roughly $2.7 \cdot 10^6$. The total birth rate for stars with masses of 1.5 - $3M_{\odot}$ is 0.26/year, with the total number of such stars in the Galaxy being $2.4 \cdot 10^8$. Thus, the fraction of main-sequence stars formed due to mergers of components due to the action of the MSW in the indicated mass interval given by the population synthesis computations is in good agreement with the fraction of Ap stars among A-type stars in a restricted volume [30]. The mass distribution for stars formed by mergers differs from a Salpeter distribution (Fig. 4). An attempt to distinguish the mass and age distributions for ordinary A and B stars and magnetic Ap and Bp stars was made, for example, in [39], but the available statistics were too poor to enable unambiguous conclusions about whether the mass and age distributions for magnetic and ordinary A and B stars are similar or different [29]. Therefore, based on the results of our population synthesis, we conclude that at least some magnetic Ap and Bp stars could be formed by mergers of main sequence stars with convective envelopes under the action of the MSW⁴;

³Here we use the simple formula $t(z) = \frac{2}{3H_0(1+z)^{3/2}}$, where t is the time since the Big Bang, z the redshift, and H_0 the Hubble constant, which in our approximate calculations is taken to be $75 \text{ km s}^{-1} \text{ Mpc}^{-1}$.

⁴We assumed that the magnetic stellar wind alters the rotational angular momentum in accordance

however, this hypothesis still awaits observational confirmation.

5 Acknowledgments

The population syntheses for close binaries for this study were carried using the “Scenario Machine” code developed by V.M. Lipunov, K.A. Postnov, and M.E. Prokhorov [32] in the Department for Relativistic Astrophysics of the Sternberg Astronomical Institute, Moscow State University.

The work was supported by the State Program of Support for Leading Scientific Schools of the Russian Federation (grant NSh-1685.2008.2, AIB; grant NSh-4354.2008.2, AVT), the Analytical Departmental Targeted Program “The Development of Higher Education Science Potential” (grant RNP-2.1.1.5940, AIB), and the Russian Foundation for Basic Research (project code 08-02-00371, AVT).

References

1. A. V. Tutukov and L. R. Yungelson, *Nauchn. Inform. Astron. Sovet Akad. Nauk SSSR* **49**, 3 (1981).
2. I. Jr. Iben, A. V. Tutukov, *Astrophys. J. Suppl. Ser.* **54**, 335 (1984).
3. W. Li, A. V. Filippenko, R. R. Treffers, A. G. Riess, J. Hu, Y. Qiu, *Astrophys. J.* **546**, 734 (2001).
4. J. Whelan, I. J. Iben, *Astrophys. J.* **186**, 1007 (1973).
5. E. Livne, *Astrophys. J.* **354**, L53 (1990).
6. E. Aubourg, R. Tojeiro, R. Jimenez, et al., eprint arXiv:0707.1328 (2007).
7. S.-C. Yoon, Ph. Podsiadlowski, S. Rosswog, *Mon. Not. Roy. Astron. Soc.* **380**, 933 (2007).
8. A. G. Riess, A. V. Filippenko, P. Challis, et al., *Astron. J.* **116**, 1009 (1998).
9. S. Perlmutter, G. Aldering, G. Goldhaber, et al., *Astrophys. J.* **517**, 565 (1999).
10. Yu. P. Pskovsky, *Sov. Astron.* **28**, 658 (1984).
11. S. Taubenberger, S. Hachinger, G. Pignata, et al., *Mon. Not. Roy. Astron. Soc.* **385**, 75 (2008).
12. G. Pignata, S. Benetti, P. A. Mazzali, et al., eprint arXiv:0805.1089, *MNRAS*, in press (2008).

with (1) in systems containing two main sequence stars with convective envelopes, when the masses of both stars are within $0.75M_{\odot}$ – $1.5M_{\odot}$. We also assumed that the matter of the components mixes totally after the merger.

13. F. K. Roepke, *Reviews in Modern Astronomy* **19**, 127 (2006).
14. G. Blanc, L. Greggio, *New Astronomy* **13**, 606 (2008).
15. B. Shustov, D. Wiebe, A. Tutukov, *Astron. Astrophys.* **317**, 397 (1997).
16. F. Förster, K. Schawinski, *Mon. Not. Roy. Astron. Soc. Lett.* **388**, L74 (2008).
17. F. Patat, P. Chandra, R. Chevalier, et al., *Messenger* **131**, 30 (2008).
18. A. V. Tutukov and L. R. Yungelson, *Astrofizika* **8**, 381 (1972).
19. D. T. Wickramasinghe, L. Ferrario, *Publ. Astron. Soc. Pacific* **112**, 873 (2000).
20. M. Nalezyty, J. Madej, *Astron. Astrophys.* **420**, 507 (2004).
21. L. Ferrario, S. Vennes, D. T. Wickramasinghe, et al., *Mon. Not. Roy. Astron. Soc.* **292**, 205 (1997).
22. S. Vennes, P. A. Thejll, D. T. Wickramasinghe, M. S. Bessell, *Astroph. J.* **467**, 782 (1996).
23. S. Vennes, P. A. Thejll, R. G. Galvan, J. Dupuis, *Astrophys. J.* **480**, 714 (1997).
24. C. Lousto, Y. Zlochower, eprint arXiv:0805.0159 (2008).
25. S. Komossa, H. Zhou, H. Lu, *Astrophys. J.* **678**, L81 (2008).
26. A. Tikhonov, *Astronomy Letters* **33**, 499 (2007).
27. V. M. Lipunov, K. A. Postnov, M. E. Prokhorov, *Astron. Astrophys.* **310**, 489 (1996).
28. V. M. Lipunov, K. A. Postnov, M. E. Prokhorov, *Mon. Not. Roy. Astron. Soc.* **288**, 245 (1997).
29. P. North, J. Babel, D. Erspamer, *Contrib. Astron. Obs. Skalnaté Pleso* **38**, no. 2, 375 (2008).
30. J. Power, G. Wade, M. Aurie're, J. Silvester, D. Hanes, *Contrib. Astron. Obs. Skalnaté Pleso* **38**, no. 2, 443 (2008).
31. A. G. Masevich and A. V. Tutukov, *Star Evolution: The Theory and Observations* (Nauka, Moscow, 1988) [in Russian].
32. V. M. Lipunov, K. A. Postnov, M. E. Prokhorov, *Astrophysics and Space Physics Reviews* **9**, 1 (1996, *The Scenario Machine: Binary Star Population Synthesis*, Eds. R. A. Sunyaev, Harwood academic publishers).
33. V. M. Lipunov, K. A. Postnov, M. E. Prokhorov, A. I. Bogomazov, accepted by *Astron. Rep.*, eprint arXiv:0704.1387 (2007).
34. A. I. Bogomazov, M. K. Abubekerev, and V. M. Lipunov, *Astron. Rep.* **49**, 644 (2005).

35. E. P. J. van den Heuvel, in S. N. Shore, M. Livio, E. P. J. van den Heuvel, *Interacting Binaries*, p. 103, Springer-Verlag, (1994).
36. E. P. Kurbatov, A. V. Tutukov, and B. M. Shustov, *Astron. Rep.* **49**, 510 (2005).
37. G. Valyavin, S. Fabrika, *ASP Conference Series* **169**, 206 (1999).
38. X. Meng, X. Chen, Z. Han, eprint arXiv:0802.2471 (2008).
39. S. Hubrig, P. North, G. Mathys, *Astrophys. J.* **539**, 352 (2000).

Figure captions

Figure 1: The mass distribution for WDs that have not undergone mergers (solid curve) and the total mass distribution for merging WDs (dash-dotted curve). The horizontal axis plots the mass of the WD in M_{\odot} (the total mass of the two WDs in the case of merging WDs), and the vertical axis the number of WDs (and of mergers) derived from the calculations. Graph (a) corresponds to all types of chemical compositions of WDs, (b) to helium WDs, (c) to carbon-oxygen WDs, (d) to oxygen-neon WDs, and graph (e) presents the total mass distribution for merging WDs of various chemical compositions. In graph (e), α denotes ONe+CO, β ONe+He, and γ CO+He.

Figure 2: The average mass of merging WDs as a function of time from the onset of the star formation. The numbers at the top mark the curves corresponding to mergers of 1 all WDs, 2 WDs of all possible chemical compositions, but taking into account only mergers in which the total mass of the WDs exceeds the Chandrasekhar limit, 3 carbon-oxygen WDs, and 4 carbon-oxygen WDs with the total mass exceeding the Chandrasekhar limit. The following assumptions for the star formation history were made: (a) all stars in a galaxy were formed at the same initial time, (b) the star formation rate has been constant, (c) the star formation history corresponds to that in [36].

Figure 3: Distribution of the lifetime from the formation of a binary system consisting of two CO dwarfs to their merger (SN Ia explosion), for carbon-oxygen WD binaries with total masses exceeding the Chandrasekhar limit.

Figure 4: Mass distribution for main sequence stars formed in mergers of main sequence stars with convective envelopes under the action of the magnetic stellar wind.

Table 1: Birth and merger rates for various types of WD, and rates of mergers of WDs with NSs and BHs, calculated for various efficiencies of the common envelope stage α_{CE} , per year in the Galaxy.

Event \ α_{CE}	0.3	0.5	1.0
He+He ¹	0.016	0.015	0.011
He+Any ²	0.066	0.08	0.1
CO+CO ¹	$4.7 \cdot 10^{-3}$	$4.8 \cdot 10^{-3}$	$4.4 \cdot 10^{-3}$
CO+CO ^{1,3}	$1.9 \cdot 10^{-3}$	$1.9 \cdot 10^{-3}$	$1.8 \cdot 10^{-3}$
CO+Any ²	0.49	0.49	0.5
ONe+ONe ¹	$1.1 \cdot 10^{-4}$	$4.7 \cdot 10^{-4}$	$7.7 \cdot 10^{-4}$
ONe+Any ²	0.004	$4.7 \cdot 10^{-3}$	$5.4 \cdot 10^{-3}$
ONe+He ¹	$3.5 \cdot 10^{-5}$	$6 \cdot 10^{-5}$	$2.8 \cdot 10^{-4}$
CO+He ¹	0.006	$8.5 \cdot 10^{-3}$	$8.2 \cdot 10^{-3}$
ONe+CO ¹	0.002	$2.4 \cdot 10^{-3}$	$1.8 \cdot 10^{-3}$
NS+WD ¹	$4.7 \cdot 10^{-4}$	$4.7 \cdot 10^{-4}$	$6.1 \cdot 10^{-4}$
BH+WD ¹	0	$1.5 \cdot 10^{-6}$	$3.7 \cdot 10^{-6}$

¹Merging of corresponding objects.
²Formation of corresponding systems.
³The total mass of the merging dwarfs exceeds the Chandrasekhar limit.

Table 2: Rates for mergers of NSs with NSs and BHs calculated for various kick velocities obtained during the formation of the NSs (v_0) and (v_0^{bh}), per year in the Galaxy.

Event	$v_0, v_0^{bh}, \text{ km/s}$		
	0, 0	100, 0	100, 100
NS+NS	$5.5 \cdot 10^{-4}$	$1.3 \cdot 10^{-4}$	$1.3 \cdot 10^{-4}$
BH+NS	$1.5 \cdot 10^{-4}$	$1.6 \cdot 10^{-4}$	$1.3 \cdot 10^{-4}$
BH+BH	$9.8 \cdot 10^{-5}$	$9.8 \cdot 10^{-5}$	$1.2 \cdot 10^{-4}$

The velocity of the BH was taken from (2) with v_0^{bh} , then halved.

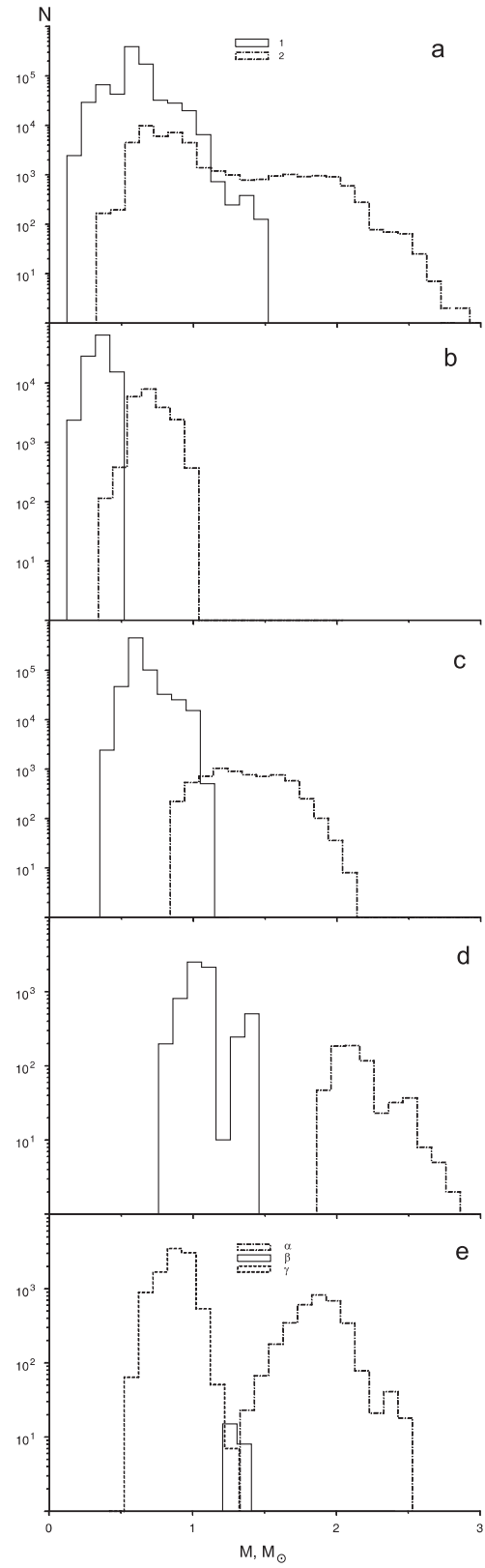


Figure 1:

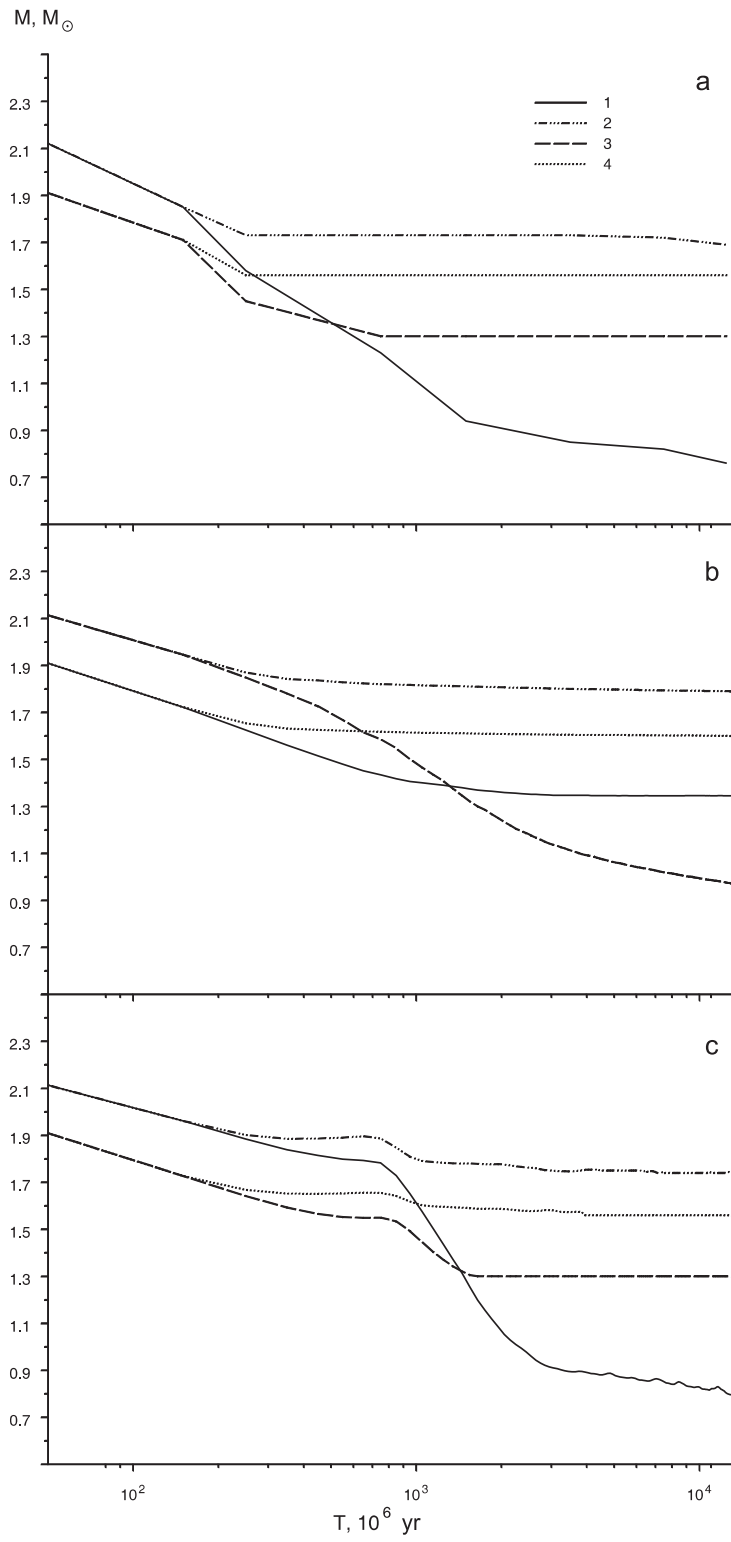


Figure 2:

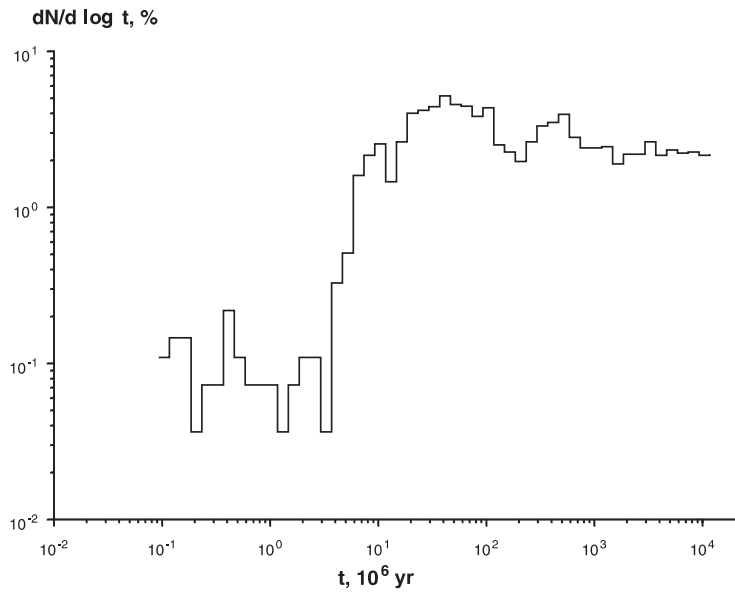


Figure 3:

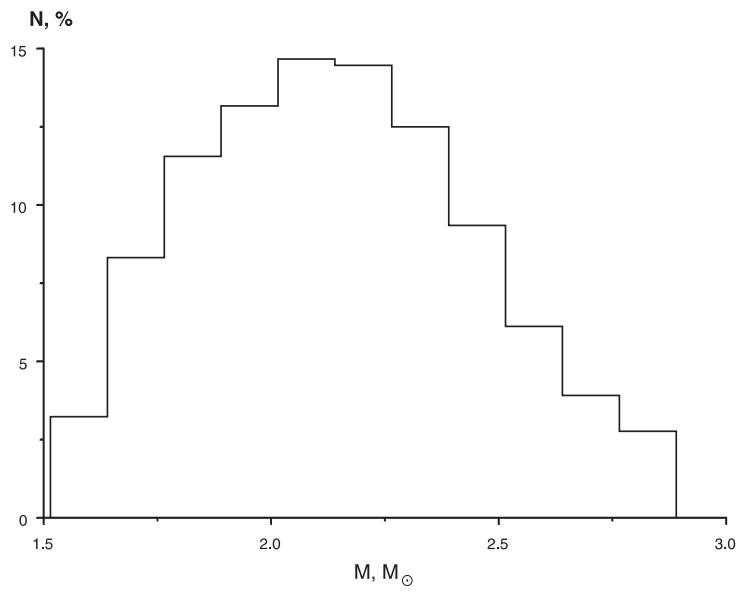


Figure 4: